energies

MDPI

Article

Cooling Strategies to Improve the Built Environment: Experimental Characterization, Model Calibration, and Multi-Climate Analysis of Innovative Ventilated and Air Permeable Roofs

Marco D'Orazio *, Arianna Latini, Andrea Gianangeli and Elisa Di Giuseppe

Department of Construction, Civil Engineering and Architecture (DICEA), Università Politecnica Delle Marche, 60131 Ancona, Italy; a.latini@univpm.it (A.L.); a.gianangeli@univpm.it (A.G.); e.digiuseppe@univpm.it (E.D.G.)
* Correspondence: m.dorazio@univpm.it

Abstract

Urban Heat Island effects and the general rise in outdoor temperatures are increasing the cooling demand in buildings. As a consequence, electrical cooling systems are becoming more common, increasing energy consumption and thus resulting in negative environmental impacts. Optimizing passive solutions that require no energy input can provide substantial benefits for building energy efficiency and urban sustainability. This study presents a research activity, financed by the EU-funded project LIFE SUPERHERO, that enhances existing roofing technologies based on passive cooling; defines an experimental method to assess their benefits in terms of energy savings; and finally evaluates their effectiveness in future climate scenarios based on greenhouse gas Representative Concentration Pathways across a set of mid-temperate/hot climate locations, also in comparison with traditional unventilated roofs. A new Climate Adaptation Efficiency Index (CAEI) was introduced to evaluate the energy efficiency potential of buildings equipped with highly ventilated and permeable clay tile roofs compared to a baseline scenario without the intervention. The results confirm the potential of ventilated and air-permeable roofs to reduce incoming heat flux and support cooling energy-efficiency planning. Indeed, CAEI values were above 20%, reaching 45–50% in hot Mediterranean and arid climates and 28–33% in cooler/temperate contexts. Under future climate scenarios, benefits further increase in the hottest Mediterranean locations, reaching up to 66%, while rising to about 44% in temperate climates, with an average increase of 10–15 percentage points, highlighting the strong potential of highly ventilated and air-permeable clay tile roofs as an effective, affordable, sustainable, and easy-to-install climate adaptation strategy.

Keywords: ventilated permeable roofs; passive cooling; model calibration; building energy efficiency

Academic Editors: Dimitrios Katsaprakakis, George M. Stavrakakis and Konstantinos Braimakis

Received: 17 December 2025
Revised: 20 January 2026
Accepted: 22 January 2026
Published: 27 January 2026

1. Introduction

The number of city residents worldwide is increasing simultaneously with soil consumption around cities [1], leading to important consequences. The process of urban expansion leads to the irreversible conversion of ecologically valuable land into impervious surfaces.

The replacement of natural surfaces with built materials modifies surface albedo, reduces evapotranspiration, and increases heat storage, thereby affecting the urban energy

balance. These processes contribute to higher near-surface air temperatures and even worse Urban Heat Island effects. In addition, urban activities such as transportation, building operation, and industrial processes introduce anthropogenic heat and air pollutant emissions, further influencing local climate conditions and air quality.

To prevent the negative consequences of uncontrolled land use, several countries have introduced strategies and policies (e.g., the EU Soil Strategy for 2030) aimed at reducing net land consumption. In the European context, the Renovation Wave initiative primarily aims at improving the energy performance and climate resilience of existing buildings through envelope retrofitting and system upgrades. Within this framework, pitched roofs and attic spaces are not systematically targeted as additional living areas, as their suitability for residential use strongly depends on building geometry, available height, and regulatory constraints. However, in specific building typologies, attics may represent underutilized spaces where specific envelope refurbishment measures can provide thermal benefits and improve summer comfort.

A recent analysis of the EU building stock (i.e., Housing in Europe 2025) indicates that more than 72% of the population living in urban areas occupies flats in multi-storey buildings [2,3]. However, attics typically require HVAC systems to maintain adequate indoor thermal conditions because of their large sun-exposed surfaces, which makes them particularly prone to overheating, especially in Mediterranean and mid-temperate climates. Rising outdoor temperatures further exacerbate this issue by increasing cooling energy demand, thus reinforcing a vicious cycle of overheating and energy consumption in urban environments. Several studies have shown that southern European regions are particularly vulnerable to overheating due to high solar irradiation, limited night-time cooling potential, and the prevalence of poorly insulated buildings constructed before the introduction of modern energy standards [4–6]. In highly urbanized Mediterranean areas such as the metropolitan areas of Barcelona, Rome, Athens, and Valencia, Urban Heat Island phenomena can further amplify cooling loads by several degrees, exacerbating indoor overheating and discomfort [7]. However, HVAC systems should not be regarded as the exclusive means for ensuring acceptable indoor environmental conditions, particularly in sun-exposed attic spaces where cooling demand tends to be significant. Although these solutions remain essential in many retrofit scenarios, they can be effectively complemented, or in some cases partially substituted, by passive technologies. These include strategies aimed at reducing heat gains, enhancing natural ventilation, or improving the thermal performance of the building envelope. Such approaches not only contribute to lowering energy demand and mitigating overheating but also support broader sustainability goals. However, the adoption of passive measures requires that their effectiveness be rigorously evaluated and quantified so that their contribution to indoor comfort and energy performance can be objectively compared with that of conventional interventions.

Passive cooling strategies aimed at reducing cooling loads are therefore essential in the transition toward climate-resilient buildings. Among these, roof-based solutions are particularly effective due to the large solar exposure of roof surfaces and their dominant role in shaping building thermal performance in conditions [8–11]. Cool roofs, reflective coatings, and green roofs have been extensively studied and deployed in Mediterranean climates, demonstrating significant reductions in peak temperatures and cooling energy demand [12–15]. However, these systems sometimes require maintenance, and in certain contexts, such as historic centres, the aesthetic alteration of the traditional pitched roof may limit their adoption [16].

On the contrary, Ventilated and Permeable Roofs (VPRs) constitute a long-established passive cooling strategy wherein a ventilated air cavity between the roof covering and the insulation layer helps dissipate absorbed solar energy [17]. Both wind-driven and

buoyancy-driven flows contribute to the ventilation rate through eaves, ridge openings, and discontinuities between tiles [18,19]. Experimental studies performed under real and laboratory-controlled conditions have highlighted the sensitivity of cavity airflow to wind speed, roof pitch, air-gap depth, and tile geometry [18]. Enhanced ventilation reduces the temperature of the outermost roof layers and limits heat transfer toward indoor spaces, effectively mitigating overheating in summer conditions.

In Mediterranean countries, pitched roofs with discontinuous clay tiles dominate the residential building stock. These coverings inherently allow a degree of airflow through side laps, head laps, and under-tile gaps. Research has demonstrated that this permeability can be exploited to enhance natural ventilation and reduce heat transfer through the roof assembly [20,21]. The air permeability of clay tiles, therefore, represents a critical parameter influencing cavity ventilation, yet it is highly dependent on tile geometry and installation details. In recent years, significant research efforts have been dedicated to improving the ventilative performance of clay tile roofs. Within the EU LIFE program, the project HEROTILE developed new tile geometries specifically designed to increase air permeability and enhance above-sheathing ventilation [22]. Full-scale experimental campaigns conducted in Italy and Israel confirmed that these modified tiles reduce deck temperatures and heat fluxes more effectively than traditional tiles, producing measurable cooling benefits even under high solar loads [20].

Building on these developments, the LIFE SUPERHERO project introduced the concept of VPR and HEROTILE-Based Roofs (HBRs), combining enhanced tile permeability with a designed ventilated cavity to maximize passive cooling performance, thus leading to the so-called "Herotiles" [23]. Preliminary findings showed that VPR systems can outperform both clay tile roofs and other passive strategies under summer conditions, with negligible operational energy use and full compatibility with traditional pitched-roof aesthetics. Despite these advances, important scientific gaps are still evident:

- The translation of laboratory-measured tile air permeability into physical parameters required for building energy simulation tools, such as discharge coefficient and effective opening area;
- The limited availability of calibrated models describing the thermal and airflow behaviour of VPR systems;
- The lack of cross-climate comparative analyses assessing VPR effectiveness in present and future Mediterranean climate scenarios.

The physical modelling of naturally ventilated cavities has been addressed by several authors. Griffith introduced a general model describing wind- and buoyancy-driven baffle ventilation, which later formed the theoretical foundation of the Exterior Naturally Vented Cavity (ENVC) model implemented in EnergyPlus [24,25]. The ENVC module enables the simulation of ventilated roof and facade systems by coupling cavity airflow, baffle temperature, and radiative and convective exchanges with the building heat balance. Accurate modelling of real discontinuous tile roofs, however, remains challenging because the airflow through multiple small under-tile openings cannot be easily represented by simple analytical expressions. Empirical discharge coefficients and effective opening areas are typically required [26]. Several studies have highlighted the need for improved methods to derive these parameters from laboratory tests or field data, especially for permeable clay tiles [20,27].

The Mediterranean basin is identified as one of the most climate-vulnerable regions worldwide. Multiple analyses predict significant increases in cooling energy demand by mid-century and the end of the century, especially under high emission pathways [28–30]. The decreasing diurnal temperature range, combined with higher minimum night temperatures, reduces the effectiveness of passive night flushing and further stresses cooling

systems. Comparative simulations show that passive roof systems, such as cool roofs, green roofs, and ventilated roofs, exhibit different resilience levels depending on future climates [31]. Yet very few studies have investigated VPR systems under future climate scenarios or across different Mediterranean climate subtypes. Understanding the long-term adaptation benefits of such systems is crucial for climate-resilient design policies.

The literature shows that ventilated and permeable roofs hold strong potential as passive cooling strategies, particularly in Mediterranean climates. However, gaps remain in translating laboratory tile permeability into EnergyPlus-ready ventilation parameters, in calibrating VPR thermal and airflow models with field data and in evaluating VPR performance across present and future climates representative of the full Mediterranean climate spectrum. The present study addresses these gaps by carrying out the following:

- Firstly, developing a machine-learning-based procedure for estimating discharge coefficients and effective opening areas from laboratory permeability tests and calibrating an ENVC-based VPR model using monitored data from a real demonstrator (see methodology in Section 2.1 and the related results in Section 3.1);
- Secondly, performing extensive iterative simulations across the Mediterranean urban context, future climate scenarios, and Representative Concentration Pathways, that describe possible future climate conditions arising from different levels of global greenhouse gas concentrations in order to quantify energy savings and climate-adaptation benefits (see Section 2.2 and the results in Section 3.2).

2. Methods

The methodology of the present research activity involved two main phases:

- Phase 1 focuses on the Building Energy Model (BEM) development and calibration, including the following: the definition of a representative residential building archetype for Mediterranean countries; the creation of a dynamic BEM in EnergyPlus based on a real case-study building corresponding to the identified archetype, where the roof is represented through the Exterior Naturally Vented Cavity (ENVC) model; the calibration of the BEM using real-time data from on-site measurements and laboratory experiments carried out within the European-funded LIFE SUPERHERO project [32,33].
- Phase 2 extends the analysis to multiple contexts and climate change scenarios: the definition of additional urban locations under Mediterranean climates; the selection of future climate change scenarios based on Representative Concentration Pathways to project future greenhouse gas concentrations; an iterative set of simulations to assess the energy benefits of the Ventilated and Permeable Roof (VPR) solution.

2.1. Development and Calibration of a Reference Building Energy Model

In an initial step, a representative residential building archetype for the Mediterranean climate was defined based on the information provided by the TABULA project [34] and the classification of the residential building stocks provided by Rosales et al. [35]. The reference building is a three-story multi-family house with a reinforced concrete structural frame and a pitched roof made of clay tiles and a wooden deck, which reflects the predominant construction practice for post-war residential blocks in Mediterranean regions. By linking the Building Energy Model (BEM) to this widely recognized typology, the calibrated simulations remain representative of a broader building stock across Mediterranean Europe.

Starting from this archetype, a detailed dynamic Building Energy Model (BEM) was implemented in EnergyPlus. Since the focus of the analysis was on the roof performance, fixed internal gains and schedules were applied by excluding occupant-driven behaviours such as window opening, artificial lighting system activation, and HVAC operation, assum-

ing a constant ventilation rate of 0.3 vol/h [36] and a constant presence of a single occupant (clothing level for summer 0.5 clo) performing light activity (sedentary, 1.2 met) [37]. The pitched roof was modelled using the Exterior Naturally Vented Cavity (ENVC) input object to model an opaque multi-skin façade or roof where an external baffle made of tiles is separated from the main roof slab by a naturally ventilated air cavity driven by wind and buoyancy forces through both edge openings (e.g., eaves and ridge vents) and distributed under-tile openings. This system, based on Griffith's theory [24], acts as a combined radiative and convective shield between the outdoor environment and the underlying roof slab surfaces. The thermal mass of the baffle is neglected, while the underlying surfaces are modelled with their own construction. The ENVC requires several input parameters including the area fraction of openings ($A_{fraction}$), the thermal emissivity and solar absorptivity of the exterior baffle material, the height scale for buoyancy-driven ventilation (ΔH_{NPL}), the effective thickness of the cavity behind the exterior baffle, the effectiveness coefficient for perforations with respect to wind (C_v), and the discharge coefficient for openings with respect to buoyancy-driven flow (C_d). These parameters are specific to the selected roof covering type.

Thus, in this study, the above-mentioned parameters were defined according to the geometric and thermo-physical properties of the roof of the LIFE SUPERHERO Project building case study, which is consistent with the identified residential archetype. Indeed, the real building demonstrator is represented by an existing multi-storey social housing building located in Reggio Emilia, a city in the north-central region of Italy. The demonstrator building with an original unventilated flat roof was renovated during the early summer of 2024 with the installation of a new attic floor covered by a pitched Ventilated and Permeable Roof (VPR) made by HEROTILE Portuguese tiles (HEROTILE-based roof, HBR) (Figure 1). Hence, it fully represents an appropriate context to support the creation of best practices for the installation of lightweight, eco-friendly attic floors in the context of global building renovations, entailing reduced covering temperature and lower summer air conditioning use.

Figure 1. Demonstrator building retrofit with HEROTILE-based roof.

The ENVC parameters were defined in two steps.

First, laboratory tests were used to determine the area fraction of openings and the discharge coefficients (C_d and C_v). One of the LIFE SUPERHERO Project's actions develops a standardized test method to assess the air permeability of VPR tiles based on British Standard BS 5534 Annex L [38] and ASTM C1570 [39] by using an airtight pressurised plenum chamber covered by an assembly of roof tiles (Figure 2). More details about the test method are described in a previous work by the authors [32].

This standardized test method was adopted to experimentally assess the air permeability of the HBR Portuguese tile installed on the building demonstrator under controlled pressure differences. The large-opening flow equations listed in the *ASHRAE Handbook Fundamentals* [40], using the measured air pressure differences and the measured volume airflow rates, were used to derive the aerodynamic area of the tile assembly ($C_{d,lab}$ A).

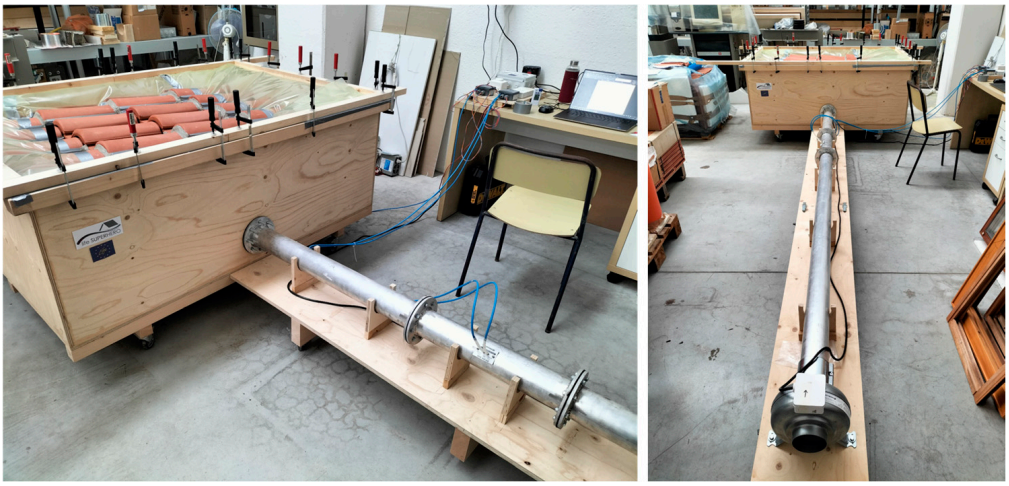

Figure 2. The laboratory setup for the characterization of roof tile air permeability.

Through additional tests on 8 reference openings with known areas, a Gradient Boosting algorithm was trained to predict the discharge coefficient $C_{d,pred}$ and effective opening area A_r. Given the rapid growth in the use of machine learning and hybrid approaches in building energy modelling, the effectiveness of data-driven methods, such as Gradient Boosting, for predicting energy consumption, estimating model parameters, and enhancing building performance simulations has been extensively highlighted [41–43]. Gradient Boosting, in particular, has demonstrated strong performance in predicting nonlinear relationships, including those governing airflow or heat transfer in building components [44–46]. In hydraulic engineering, data-driven models have been used to estimate discharge coefficients for complex flow structures, demonstrating their suitability for systems where empirical coefficients depend on complex geometries [36–38]. This is analogous to the problem of deriving discharge coefficients for permeable roof tiles.

Hence, given that the pressure range tested (1–100 Pa) encompasses both natural and forced ventilation conditions, the coefficients can be considered approximately equivalent ($C_{d,pred} \approx C_{d,lab} \approx C_v$). The $C_{d,pred}$ values were used to estimate the effective opening area of each tile and obtain the area fraction ($A_{fraction}$) input value for EnergyPlus, defined as one-half of the total area of the openings. The Gradient Boosting Model input consists of a single derived feature (i.e., $(Q_{ave}/(\Delta P_{ave} \cdot \rho)^{-1/n})$, which embeds the physical relationship between measured airflow rate, pressure difference, and flow exponent. The model was trained using a Gaussian loss function with 200 trees, an interaction depth of 4, a learning rate of 0.05, and a minimum node size of 1. Training was performed on laboratory-derived data on the 8 reference openings for which the discharge coefficients were easily determined, and the trained model was subsequently used to predict $C_{d,pred}$ for tile configurations with missing values. Model performance was evaluated using an in-sample validation approach. Model accuracy was assessed using Root Mean Square Error (RMSE) and Mean Absolute Error (MAE), together with a comparison between observed and predicted discharge coefficients. This validation strategy was adopted to verify internal consistency and the model's ability to capture the underlying relationship between the physically derived input feature and discharge coefficients given the limited size of the available dataset.

Second, an iterative calibration procedure was carried out using RStudio (v. 2023.09.1+494) [47] so that the BEM could accurately reproduce the measured thermal performance of the roof. Hybrid calibration methods that combine physics-based models with optimization or machine learning techniques have gained importance in achieving high-fidelity energy models [42,48,49]. Applying such approaches to VPR systems can substantially improve simulation accuracy and confidence in scenario-based analyses.

To this aim, data from the summer thermal performance of the roof building were adopted (Figure 3), focusing on the following:

- The roof tile outdoor surface temperature (PT100 sensors, measurement range of −50–70 °C, accuracy of ±0.15 °C) to be compared with the *Surface Exterior Cavity Baffle Surface Temperature* EnergyPlus output;
- The heat flux across the roof (measurement range: −2000–20,000 W/m^2; accuracy: ±3% of reading) to be compared with Surface Inside Face Conduction Heat Transfer Rate Per Area EnergyPlus output.

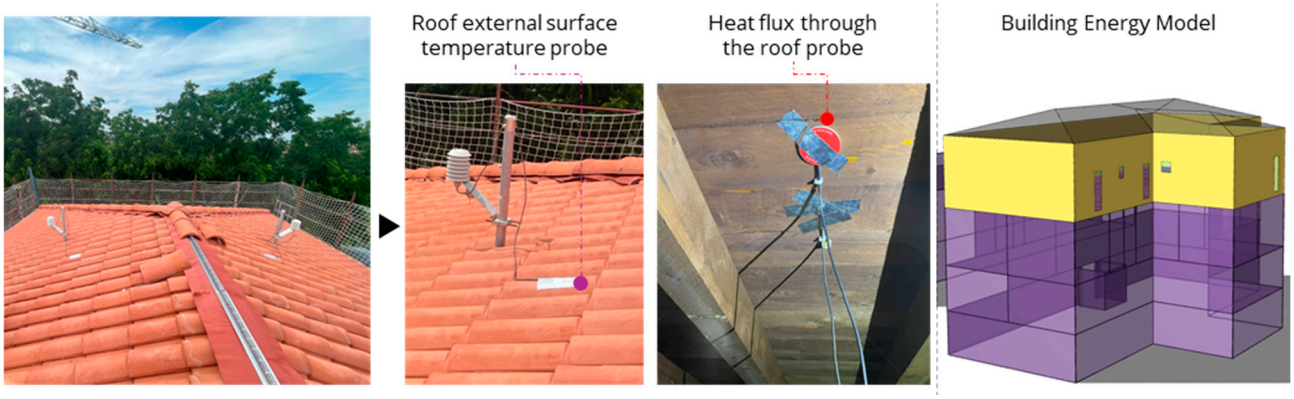

Figure 3. The monitoring system of the VPR performance on two opposite slopes (the south and the north one, 10 min data acquisition rate) and the Building Energy Model with the calibrated attic floor in yellow colour.

In addition, local outdoor climate conditions were monitored using a DAVIS Instrument WS100LRW/SR wireless LoRaWAN weather station, installed at 1.5 m above the roof of the demonstrator building. The station measures air temperature (measurement range: 40–65 °C ± 0.2 °C) and humidity (measurement range: 1–100% ± 2%); solar radiation (measurement range: 0–1800 W/m^2 ± 2%); wind speed (measurement range: 1–322 Km/h ± 5%) and direction (measurement range 0–360° ± 5°); and rainfall (measurement range 1000 mm/h ± 5%), and these data were processed to generate a local EPW file for the BEM calibration.

The iterative simulations were carried out to identify the remaining ENVC input parameters: the optimal convective heat transfer coefficient (h_c) and height scale for buoyancy-driven flow (ΔH_{NPL}), minimizing the differences between simulated and measured surface temperatures and heat fluxes. The simulation period included 57 days between 6 July and 31 August 2024. The ranges of tested parameters were 0.001–1 m for ΔH_{NPL} (s.i. 0.1) and 4–18 W/(m^{2}K) for h_c (s.i. 0.5) based on wind velocity registered in Reggio Emilia and well-established calculation methods (UNI EN ISO 6946:2018 [50], Nusselt and Jurges [51]). The BEM opaque and transparent envelope constructions features were modelled according to the geometrical and thermophysical properties of the LIFE SUPERHERO demonstrator (U_{wall} = 0.20 W/(m^{2}K); U_{window} = 1.00 W/(m^{2}K)). The simulation performance was assessed using Root Mean Square Error (RMSE) and Mean Absolute Error (MAE) metrics to achieve best-fit parameters.

2.2. VPR Benefit Assessment Across Future Climate Scenarios

To evaluate the benefits of VPR on cooling energy reduction, a set of variants of the building archetype with different VPR U-values was first created, starting from the calibrated archetype. The BEM was parametrically modified in terms of roof U-value to represent different building categories from class E (2.00–2.49 W/(m^{2}K)) to class A (0.01–0.49 W/(m^{2}K)), consistently with the U-value clusters for roofs identified

in [35]. The calibrated BEM corresponds to class E, given the presence of an uninsulated pitched roof. Higher efficiency classes (D: 1.50–1.99 W/(m^{2}K); C: 1.00–1.49 W/(m^{2}K); B: 0.50–0.99 W/(m^{2}K); A: 0.θ1–0.49 W/(m^{2}K)) were obtained by adding an EPS insulation layer to match the representative average U-value of each class. Finally, an additional A+ class was simulated, with a roof U-value equal to half of the class A value (0.01–0.24 W/(m^{2}K)), to reflect the progressive improvement in building envelope performance expected by European building retrofit policies.

A non-ventilated clay tile roof reference building was also modelled for each variant using the same ENVC module but with minimized ventilation parameters (i.e., reduced $A_{fraction}$, C_d, and C_v). This configuration represents a clay tile roof assembly with negligible air permeability, such as roofs where the under-tile cavity is partially or fully obstructed (e.g., by mortar or construction practices that inhibit air flow), rather than an intentionally ventilated roof system.

All the above-mentioned building variants were then applied to a set of additional urban contexts under Mediterranean climates, where the cooling demand is typically high. Based on the groups of the Köppen–Geiger climate classification, the following Mediterranean cities were selected:

- BWh (hot desert-arid climate): Alicante.
- BSk (cold semi-arid climate): Madrid, Zaragoza.
- BSh (hot semi-arid climate): Valencia; Lefkosa.
- Cfa (temperate climate with hot summer and without dry season): Bologna and Ljubljana.
- Csa (temperate climate with dry and hot summer): Palermo, Rome, Sevilla, Athens, Nice, and Zadar.
- Csb (temperate climate with dry and warm summer): Santiago de Compostela.

Weather files (EPW) based on Typical Meteorological Years (TMYs [52]) for each city were used to perform simulations using the calibrated reference building model in EnergyPlus in the summer season (120 days, from 1 June to 30 September). The use of TMYs provides a standardized and representative climatic dataset, widely adopted in building performance simulation, to ensure internal consistency across the analysed scenarios. In addition, the corresponding future weather files were created using Future Weather Generator at a mid-century projection (i.e., central year at 2050) and end-century projection (i.e., central year at 2080) and with Representative Concentration Pathways (RCPs): 2.6, 4.5, and 8.5. RCP scenarios represent increasing levels of climatic stress on buildings, from moderate warming with a stringent mitigation scenario (RCP 2.6) to severe warming with very high GHG emissions (RCP 8.5) [29], and are used here to assess how the adaptation benefits of VPR-HBR strategies evolve over time.

In summary, the analysis considered 6 building U-value variants with VPR and with a non-ventilated clay tile roof, which were simulated in 14 cities and 7 time scenarios (TMY, future climates for 2050 and 2080 for each RCP), resulting in a total of 1176 simulations, which were run iteratively through a combined EnergyPlus and RStudio (v. 2023.09.1+494) workflow.

For each simulated scenario, the EnergyPlus output variable Surface Inside Face Conduction Heat Transfer Rate Per Area was exported, and the authors denoted the heat flux through the non-ventilated roof configuration by Q_{NV} and the corresponding flux through the HBR configuration by Q_V.

Finally, a Climate Adaptation Efficiency Index (CAEI) was defined and calculated to quantify the VPR benefit. In particular, CAEI expresses the relative energy efficiency potential of the roof equipped with the VPR-HBR solutions compared to a baseline scenario without the intervention (TMY). The indicator specifically accounts for heat gains transmitted through the roof to the attic thermal zone and does not represent the overall energy

performance of the entire building. Other relevant contributors to summer heat gains (e.g., air exchange rates, solar radiation through transparent elements) are intentionally excluded in order to isolate the effect of the roof system. As a result, CAEI was conceived as a roof-level relative performance indicator. Three CAEIs were calculated to quantify the relative reduction in incoming thermal heat fluxes at the reference climate ($CAEI_{TMY}$, see Equation (1)) and under future climate conditions in 2050 ($CAEI_{2050}$, see Equation (2)) and 2080 ($CAEI_{2080}$, see Equation (3)), thereby indicating the adaptive benefit provided by the VPR:

$$CAEI_{TMY} = \frac{\sum Q_{NV,\,TMY} - \sum Q_{V,\,TMY}}{\sum Q_{NV,\,TMY}}\ [\%] \quad (1)$$

$$CAEI_{2050} = \frac{\sum Q_{NV,\,2050} - \sum Q_{V,\,2050}}{\sum Q_{NV,\,TMY}}\ [\%] \quad (2)$$

$$CAEI_{2080} = \frac{\sum Q_{NV,\ 2080} - \sum Q_{V,\,2080}}{\sum Q_{NV,\ TMY}}\ [\%] \quad (3)$$

The VPR-HBR benefit assessment based on CAEI involved both a within-climate and between-climate analysis. Within each climate, CAEI values are used to quantify the relative impact of roof ventilation across insulation levels and future scenarios, using TMY conditions as a consistent reference baseline. In addition, CAEI trends are compared between climates to investigate the relative effectiveness of the VPR-HBR system across different contexts, ensuring a consistent interpretation despite differing climatic boundary conditions.

3. Results

This section presents the results in two main parts to reflect the multi-step approach of the present research activity:

- Section 3.1 reports the outcomes of the BEM calibration, including the estimation of the HEROTILE parameters obtained by the Gradient Boosting Machine model for their implementation in the Exterior Natural Vented Cavity Energy Plus module. Then, the results of the iterative calibration of the dynamic Building Energy Model (BEM) are reported, demonstrating the ensuring consistency between simulated and measured heat fluxes and external roof surface temperature.
- Section 3.2 presents the benefit assessment of the VPR-HBR under current and future climatic conditions, depending on the building variants investigated. First, the results under the TMY dataset are discussed, highlighting the thermal and energy benefits of the VPR-HBR compared to a conventional non-ventilated roof. Subsequently, the benefits during future climate scenarios are analysed to evaluate how the magnitude of the HBR benefits evolves across different Representative Concentration Pathways and time horizons. While the Climate-Adaptive Energy Index is used in this study as a normalized indicator to enable consistent comparisons across roof classes, climates, and scenarios, the corresponding heat gain values for both ventilated and non-ventilated configurations are also provided in the Supplementary Materials.

3.1. Reference Building Energy Model Calibration

Concerning the GBM, the algorithm achieved very high predictive accuracy, with an RMSE of 6.9×10^{-5} and a MAE of 5.9×10^{-5} on the training dataset, indicating an excellent fit between simulated and observed discharge coefficients (see Figure 4).

Thanks to this significant accuracy level, the proposed workflow enabled the reliable estimation of the discharge coefficient ($C_d \approx C_v = 0.71$) for the Portuguese HEROTILE installed on the building demonstrator and consequently allowed the calculation of the corresponding effective area fraction ($A_{fraction} = 0.0244$).

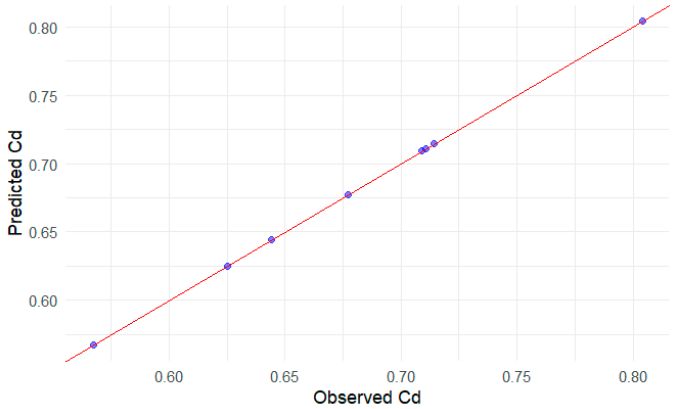

Figure 4. Prediction accuracy of the Gradient Boosting Machine on the training set to predict discharge coefficients.

In total, 145 iterative simulations were performed for the BEM calibration, adopting fixed ENVC parameters concerning roof tile absorptivity (0.59), emissivity (0.84), and air gap thickness (0.08 m), based on the real values of the installed HEROTILES.

The best-performing configuration was obtained with an area fraction of openings equal to 0.0244, an external convective heat transfer coefficient of h_c = 18 W/(m^{2}K), and a neutral pressure-level height difference of ΔH_{NPL} = 0.001 m.

This setup led to an RMSE and MAE between measured and simulated roof surface temperature of 5.87 K and 3.75 K, respectively, with a maximum temperature difference equal to 0.89 °C. Concerning the heat flux, the corresponding RMSE and MAE were 6.10 W/m^2 and 4.23 W/m^2, with a maximum absolute flux difference of 1.24 W/m^2.

Figure 5 reports the trend in simulated and measured heat flux and outdoor roof surface temperature for the best detected simulation, highlighting a very strong correspondence between the results and reliability of the iterative combined EnergyPlus-RStudio (v. 2023.09.1+494) process.

3.2. VPR Benefits Assessment Across Future Climate Scenarios

3.2.1. TMY Scenario

Concerning the outcomes at TMY, the Climate Adaptation Efficiency Index shows a clear dependence on both the building variants and the climatic context (Figure 6).

In general, the results are promising, since CAEI remains above 18% in all cities and buildings, meaning that the VPR-HBR solution provides a significant reduction in incoming heat through the roof compared with a non-ventilated roof, even in the absence of roof insulation (class E). The benefits are more pronounced in Csa and BWh climates for all building variants, confirming that in the hottest Mediterranean conditions, the effectiveness of the VPR-HBR solution is maximized.

More specifically, the results reveal some systematic trends across building variants:

- From class E (uninsulated VPR-HBR) to class A (≈0.10 m of insulation layer), the CAEI increases for every city and climate. Indeed, the benefit increases on average by +5 percentage points for a class B roof compared with the uninsulated-roof class E and reaches about +10 percentage points for a class A roof.
- As expected, the maximum benefit is obtained for class A, where CAEI values typically range from 28 to 33% in cooler/temperate contexts (i.e., Cfa, Csb) up to 45–50% in hot Mediterranean and arid climates (i.e., Csa, BWh);
- Interestingly, in the A+ configuration (≈0.22 m of insulation layer), the CAEI decreases again, and the index is more similar to class B than to class A. This indicates that the benefits of the VPR-HBR solution are maximized for a standard insulated roof while

using a super-insulated roof does not provide additional adaptation gains and can even reduce the relative impact of the ventilated roof technology.

These outcomes are consistent across all cities.

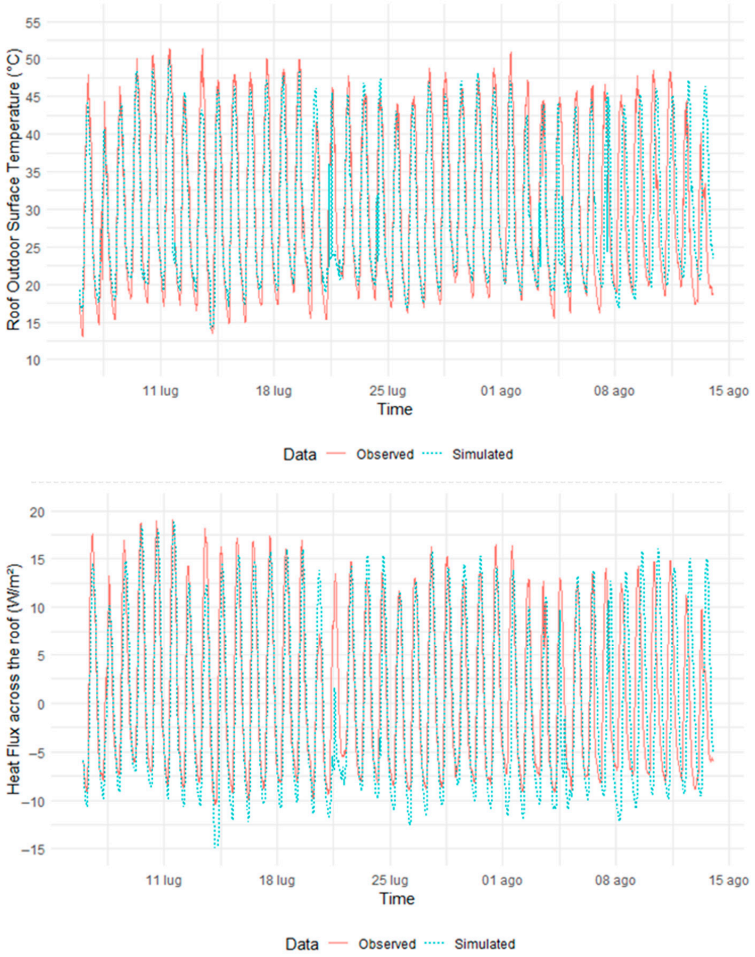

Figure 5. Trends comparison between observed data and best simulation results.

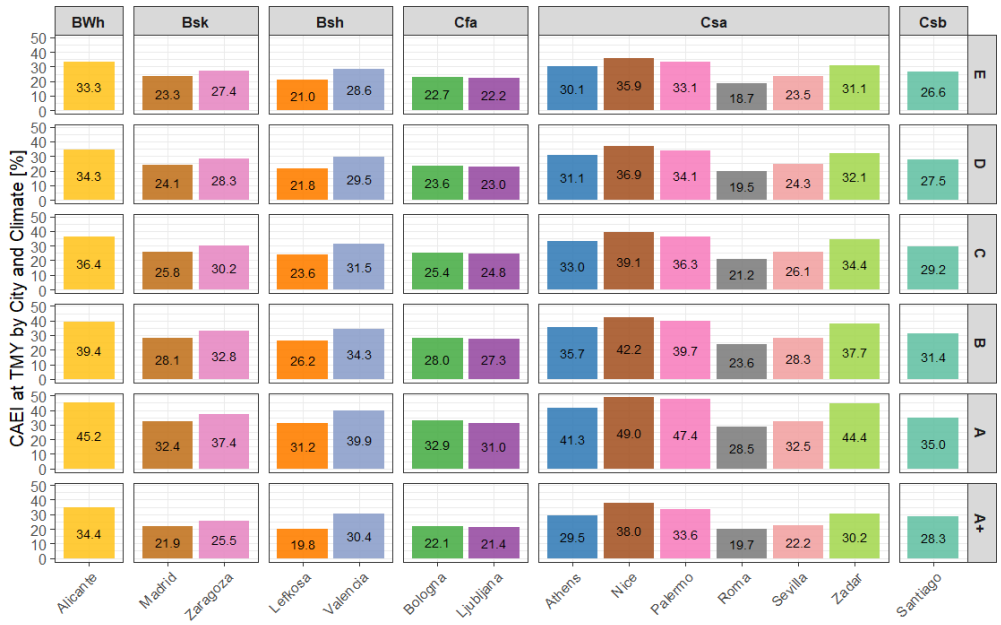

Figure 6. Histograms of CAEI values across climates, cities (represented by different colours) and building variants at TMY.

The subsequent sections analyse how the benefits of the VPR-HBR roof evolve under future climate conditions by comparing the CAEI across different RCP-based scenarios and time periods.

3.2.2. Climate Change RCP 8.5 Scenario (Worst Scenario)

When comparing the TMY baseline with the high-emission RCP 8.5 scenario, a consistent trend emerges across all cities and building classes. The slope of the lines (Figure 7) shows that the increase in CAEI between TMY and 2050 is the most pronounced, whereas the additional gain between 2050 and 2080 tends to reach a steady state. This indicates that the marginal benefits of the VPR-HBR solution grow rapidly in the near future, but the solution is able to maintain its benefits as climatic conditions become more extreme, demonstrating a stable adaptation potential over time.

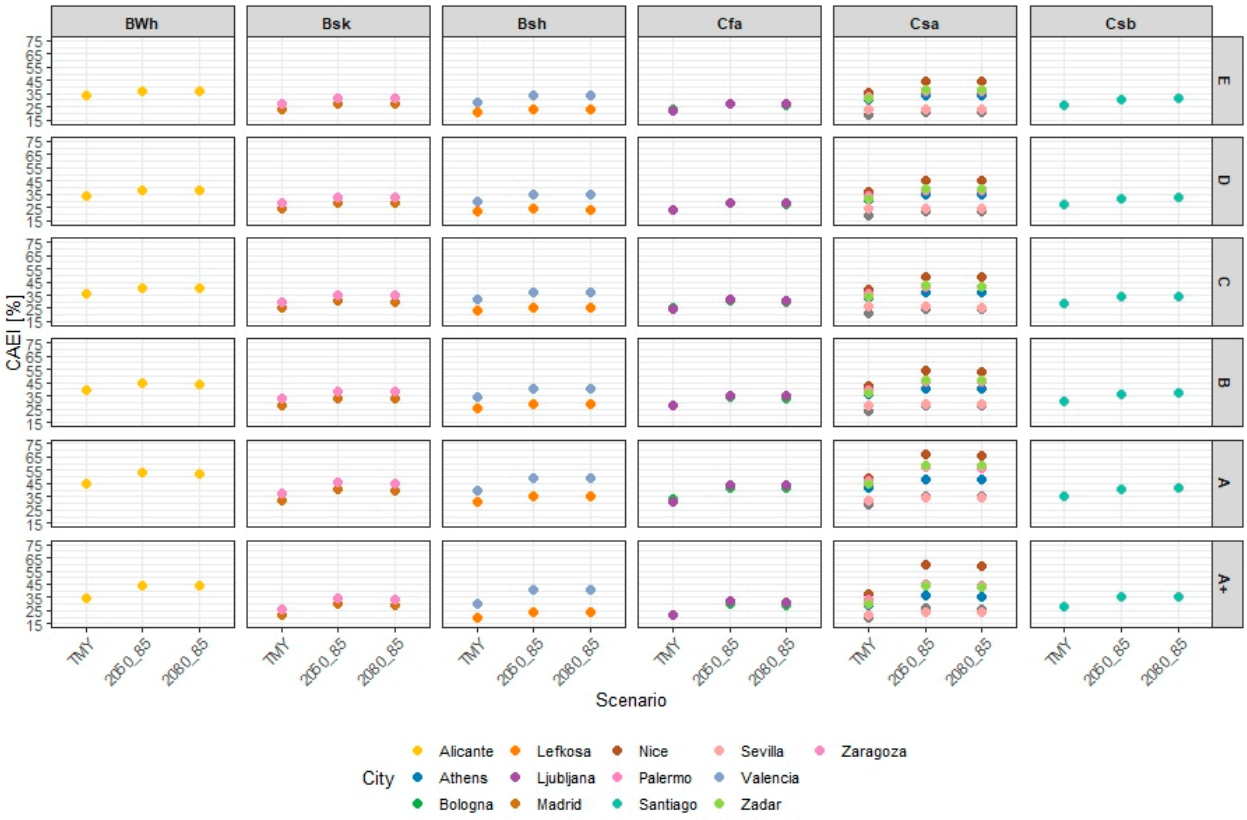

Figure 7. Trend in CAEI for RCP 8.5 Scenario across TMY, 2050, and 2080 for each climate and building variant; "2050" and "2080" indicate the central reference years of mid-century and end-century climate projections, respectively.

Across the full set of simulations, CAEI values are very high, with values always above 20%, confirming the robustness of ventilated roofs even under evolving climatic conditions. In particular, the larger benefits are concentrated in the hottest Mediterranean locations (i.e., BWh, Csa), with coastal cities such as Alicante, Nice, Palermo, and Zadar consistently exhibiting the highest CAEI values commonly between 37 and 66%. This outcome confirms that, in this climate, the adaptation potential of the VPR-HBR roof is maximized. The combination of a high baseline cooling demand and the enhanced effectiveness of VPR-HBR in limiting heat gains under severe warming conditions makes these retrofit strategies particularly advantageous. More temperate climates and cold steppe–arid climates, such as Cfa, Csb, and BSk, display a moderate positive increment (26–44%), though the VPR-HBR solution still delivers robust CAEI values across the full range of building classes.

This pattern is consistent for all building variants: moving from E to B and A classes, the CAEI increases in every climate, meaning that the intensification of summer temperatures amplifies the cooling need for buildings, thereby enhancing the relative energy benefit of VPR compared to non-ventilated roofs.

The interesting exception remains the A+ class, where CAEI values are systematically lower than class A and closer to class B for all climate and future time scenarios (except for the Nice location).

3.2.3. Climate Change RCP 4.5 Scenario (Intermediate Scenario)

Under the RCP 4.5 scenario, the performance of the VPR-HBR roof shows a clear and consistent pattern across all buildings and cities: Benefits increase moderately from TMY to 2050 and then remain stable toward 2080 (Figure 8). This reflects the results already highlighted for RCP 8.5, indicating that, despite progressively warmer summers, VPR continues to offer meaningful cooling-energy advantages even under a moderate stabilized warming trajectory.

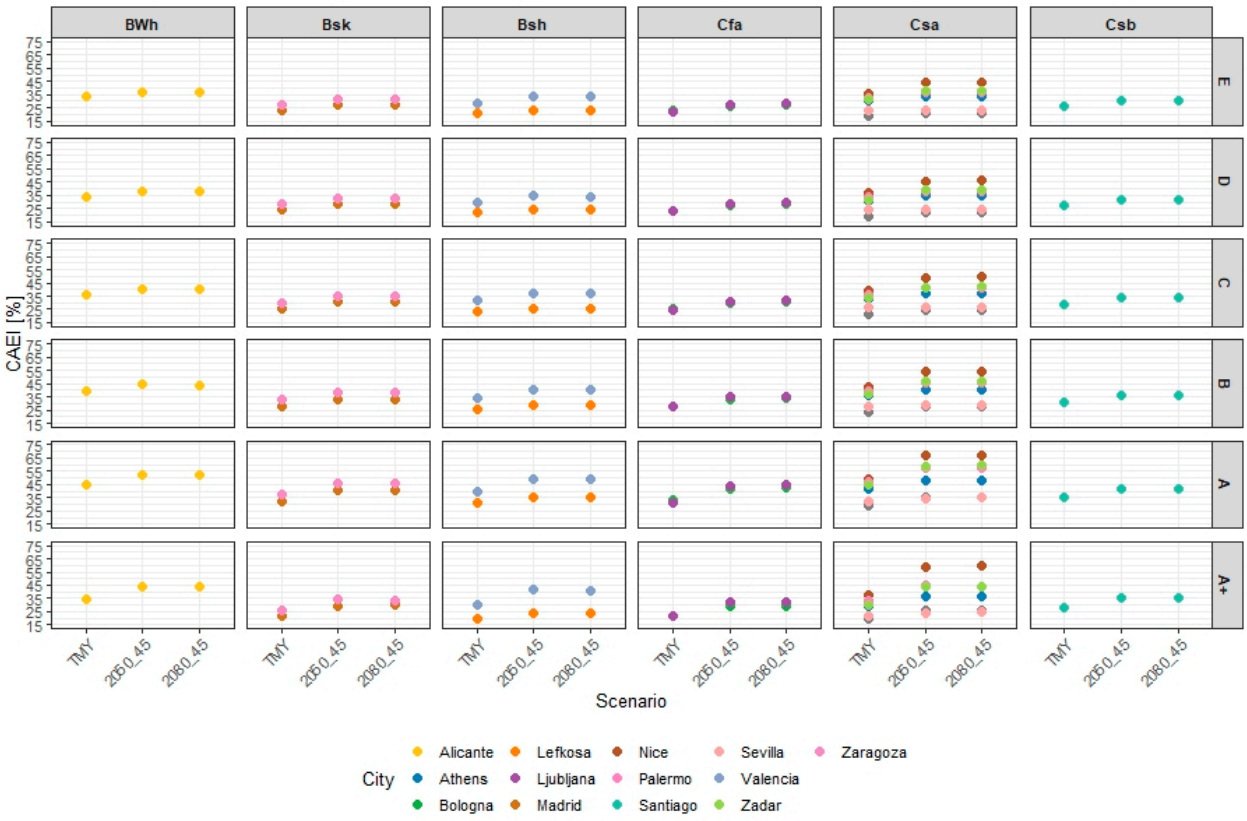

Figure 8. Trend in CAEI for RCP 4.5 Scenario across TMY, 2050, and 2080 for each climate and building variant; "2050" and "2080" indicate the central reference years of mid-century and end-century climate projections, respectively.

The CAEI values obtained under RCP 4.5 are generally around two percentage points higher compared to the RCP 8.5 scenario. This indicates that the VPR-HBR system performs even more effectively in a stabilization pathway where future summer warming is expected to face less extreme thermal stress, enhancing the roof ventilation-driven cooling potential.

As already observed for TMY and for RCP 8.5 scenarios, the strongest benefits emerge in hot-summer Mediterranean (Csa) and hot arid or semi-arid climates (BWh, Bsh), particularly in coastal cities. Indeed, city-level variability is significant within these climates: Locations such as Nice, Zadar, Palermo, Alicante, and Valencia consistently reached up to 50–67% CAEI, displaying a higher adaptation efficiency, while Sevilla, Roma, and Valen-

cia remain in a moderate range (20–35%) despite sharing the same Köppen classification. This difference can be attributed to climatic factors including diurnal temperature variations, wind patterns, humidity, and local irradiance, which influence the effectiveness of air movement in under-tile ventilation and above-sheathing ventilation between tile layers. On the other side, milder climates, such as Cfa and Csb, show moderate but reliable gains (27–44%).

A consistent trend is also evident across building variant classes, with class A buildings showing the highest benefits, while class A+ is approximately 10 percentage points lower, approaching class B, with an evident exception for Nice. At TMY, the A+ class in Nice exhibited a lower benefit than class A and a performance comparable to class B. In future scenarios, however, the increase the effectiveness of ventilation is evident even in super-insulated buildings: A+ remains about 5 percentage points below class A but consistently outperforms class B, suggesting that climate warming enhances the effectiveness of the VPR-HBR solution even where insulation levels are already very high.

3.2.4. Climate Change RCP 2.6 Scenario (Best Scenario)

The comparison between CAEI values at TMY and the low-emission RCP 2.6 scenario highlights a consistent temporal pattern across all cities and building classes (Figure 9). Indeed, CAEI values rise evidently between TMY and 2050, with a lower increasing rate (typically by 0.5–1 percentage point) between 2050 and 2080, indicating that the incremental adaptation benefit of the VPR-HBR roof is robust also towards more severe warming scenarios.

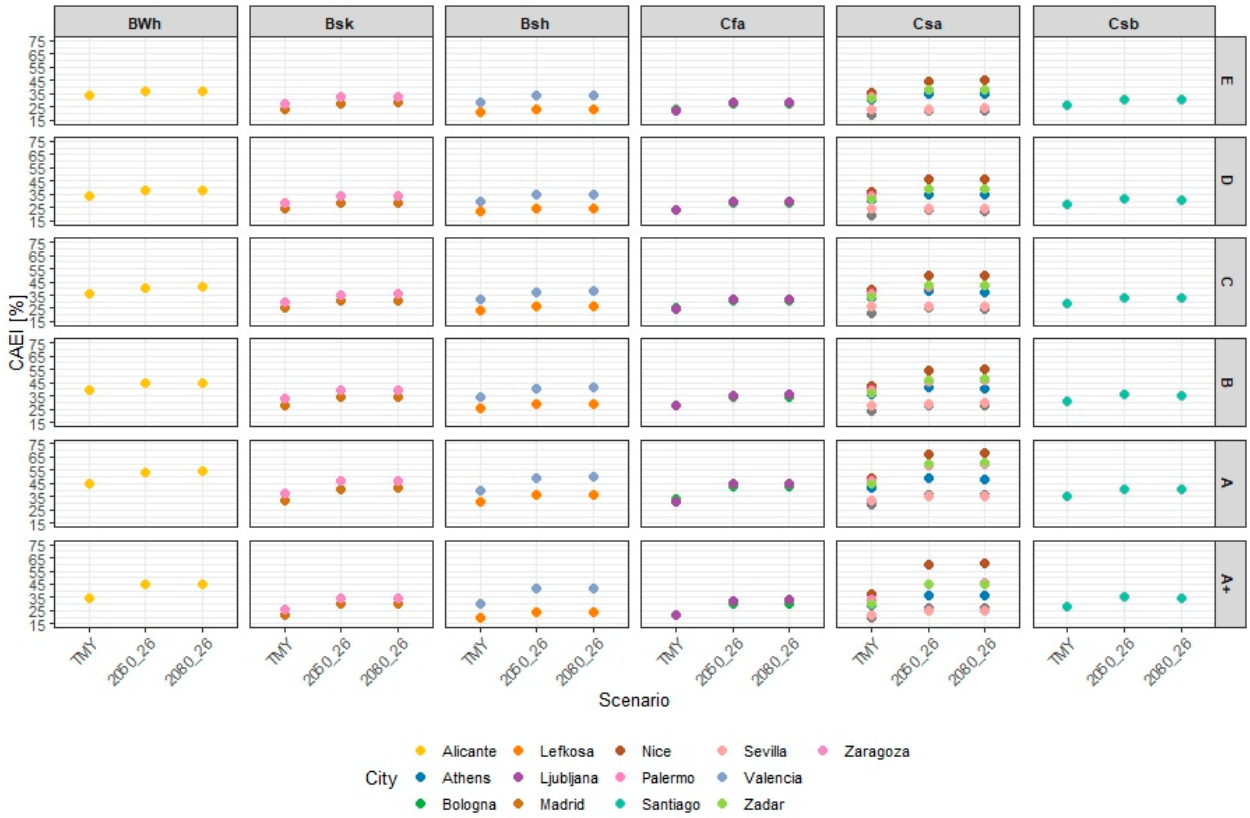

Figure 9. Trend in CAEI for RCP 2.6 Scenario across TMY, 2050, and 2080 for each climate and building variant; "2050" and "2080" indicate the central reference years of mid-century and end-century climate projections, respectively.

Overall, RCP 2.6 presents a scenario of modest climatic intensification in which VPR-HBR performance maintains high efficiency, with the strongest benefits persist-

ing in Mediterranean hot-summer and hot desert/semi-arid contexts (Csa, BWh/BSh). Coastal cities already characterized by high baseline CAEI values in the TMY and RCP 8.5 and 4.5 achieve the highest results also in RCP 2.6, with values reaching ~68% in class A for Nice, ~59% in Palermo, ~60% in Zadar, and 53% in Alicante.

Building variants confirmed the expected hierarchy with a correspondence between increasing roof-insulation levels and increasing CAEI values: Standard-insulated buildings (i.e., A, B) experience the highest CAEI up to 68%, but even the least insulated configuration (class E) exhibits very positive CAEI values around 45% (Nice) and 38% (Palermo, Zadar, and Alicante) in a hot climate and intermediate values (20–30%) in more temperate climates (Cfa and Csb). Conversely, super-insulated buildings (A+, ~24–60%) exhibit, on average, 10-point percentage smaller but still positive increments compared to class A (~35–68%), with the exception of Nice, confirmed as previously observed for RCP 8.5 and 4.5.

4. Discussion

In this section, the outcomes presented in the previous paragraph are discussed with special attention to the analysis of climatic influences, future scenarios, and RCP trends; the influence of building roof-insulation variants; the presence of cross-city variability; and the identification of the design and adaptation implications of the VPR-HBR roofing system.

A cross-scenario analysis highlights several main findings by first considering the climate-dependent performance of the VPR-HBR with the highest adaptation benefits concentrated in the more cooling-demanding contexts. In general, Climate Adaptation Efficiency Index (CAEI) outcomes proved this solution to be promising across all considered climatic contexts and time scenarios compared to a conventional non-ventilated roof, indicating that the improved ventilation effects consistently reduce heat transfer across the roof, offering tangible benefits as a passive solution. More specifically, the reduction in incoming heat flux across the roof, thanks to VPR-HBR, is consistently maximized in Mediterranean hot-summer and hot desert/semi-arid contexts (Csa, BWh/BSh). These locations exhibit more intense summer solar heat gains through higher outdoor air temperatures, with VPR-HBR providing a very high adaptation benefit, enhancing the potential of cooling energy use reduction. This confirms that the intrinsic capacity of VPR to reduce heat gains becomes increasingly effective where cooling loads are naturally higher and where the roof contributes significantly to building overheating. In more temperate climates (Cfa and Csb), there were still substantial moderate benefits due to moderate cooling needs and more uniform summer conditions.

Second, building variants in terms of simulated roof U-value variations confirmed an expected hierarchy, with increasing insulation shifting the magnitude of the CAEI upwards, resulting in more benefits in comparison with the same insulated-level non-ventilated roof. Specifically, across all climates and time scenarios, VPR-HBR combined with moderate insulation layers (e.g., class A, 0.01–0.49 W/(m^{2}K)) already maximizes climate adaptation benefits, reducing the incoming heat gains. This highlights a synergistic relationship between envelopes and passive cooling strategies: As the building envelope becomes more efficient, the contribution of VPR becomes proportionally more significant. Conversely, in extremely highly insulated buildings, as simulated in class A+, fewer benefits are observed, and this may also result in unnecessary material and economic costs, indicating that VPR-HBR delivers the maximum value in standard-insulated buildings and that roof-insulation beyond a certain threshold does not amplify the cooling benefit. This underscores the importance of avoiding over-insulation when passive cooling strategies are adopted as a building retrofit measure, confirming the previous literature pointing out that there exists a point where a building switches from pro-insulation to anti-insulation [53], resulting in higher energy consumption [54] even in cold climates [55]. Future work will

extend the present analysis by quantitatively linking roof ventilation effectiveness to key climatic drivers in order to strengthen the physical interpretation of the observed CAEI trends and the anti-insulation effect under different climate conditions. Such an approach would enable the identification of climate-dependent thresholds beyond which ventilation becomes less effective in highly insulated envelopes and would support the development of climate-specific design guidelines for ventilated roofing systems.

Third, a great improvement of VPR-HBR benefits under future climate conditions, coupled with a marked stability of performance between 2050 and 2080, emerged. Across all building classes, climatic contexts, and Representative Concentration Pathways, the largest and most evident increase in CAEI occurs between TMY and 2050, reflecting the stronger response of the VPR-HBR solution to the initial phase of climate warming, with most of the adaptation potential unlocked by mid-century. Between 2050 and 2080, the achievable benefit consolidates in a stable trend with a 1–2 percentage point increase, representing a positive signal. Even under very severe warming with peak temperatures intensifying and a more prolonged cooling season, the VPR-HBR strategy maintains its adaptation potential, highlighting its resilience and long-term suitability for climate-responsive building design in Mediterranean and warm climates, even as climatic severity continues to evolve. In addition, the comparison among RCPs in future climate scenarios reveals that, under the RCP 2.6 pathway, the CAEI is generally 1–2 percentage points higher than in the intermediate (RCP 4.5) and high-emission (RCP 8.5) scenarios, respectively. This can be explained by the fact that, under a strong mitigation scenario, summer conditions become warmer but do not reach the most extreme levels, and in this condition, the VPR-HBR operates in an optimal range at which passive ventilation effects can be more exploited.

These considerations are generally valid across all simulated building variants and climatic contexts, confirming the robustness of the VPR-HBR solution under different global warming trajectories. However, some differences among cities belonging to the same Köppen–Geiger classification emerged. For example, in the Csa group, Nice, Zadar, and Palermo exhibited significantly higher benefits compared to Sevilla and Valencia, which achieved slightly lower CAEI. This may be attributed to the fact that the Köppen–Geiger groups are macro-climatic labels [56–58] that do not capture key local factors, such as cloudiness and wind patterns affecting ventilation in the cavity. These are particularly important factors affecting heat gains through the roof and a more favourable condition for natural ventilation in the cavity. As a result, this variability within the same climate class highlights the need for site-specific assessments, as broad climatic categories alone cannot predict the actual effectiveness of VPR-HBR solutions in each specific location.

Given the interactions between climate, envelope characteristics, and achieved VPR-HBR benefits in comparison with a non-ventilated roof building, the importance of reinforcing pre-retrofit and pre-design assessments using advanced models and tools to shape climate-specific building retrofit is highlighted. Such analyses can help identify the optimal configuration between envelope features and ventilated roof performance, avoiding unnecessary material and economic costs and also reducing the embodied and life-cycle impacts associated with excessive insulation, while still maximizing cooling demand and climate adaptation benefits.

In this context, the workflow and the automated simulation tool presented in this study demonstrated their suitability in testing hundreds of configurations across many climates, obtaining reliable results in future climate warning assessments. The method provides a scalable framework for expanding analyses to additional contexts, building types, and other passive cooling technologies (e.g., VPR-HBR with Marseille tiles), supporting broader adoption of pre-retrofit assessment of tailored climate-adaptive solutions.

To complement the above discussion, the following points highlight the main limitations of the present study. From a methodological point of view, the present study uses a single climate file as input for the generation of a file for future scenarios, which may not capture the full range of variability projected by different climate models. However, the selected Typical Meteorological Year provides a standardized and representative dataset, ensuring methodological reproducibility and allowing the approach to be extended to multiple locations, scenarios, or alternative climate data sources in future studies.

It is also important to recognize the relatively limited size of the training dataset used in the machine learning model to determine the discharge coefficients, which may affect generalizability and increase prediction uncertainty. Nevertheless, the dataset is based on high-quality data measured through a standardized test method [32] derived from well-established British Standard BS 5534 Annex L [38] and ASTM C1570 [39], resulting in overall high accuracy. Future work could expand the training dataset by testing a wider range of reference openings with known areas to further improve generalizability.

Moreover, the analysis is based on a single building archetype, which allows a controlled and systematic comparison across climates, insulation levels, and future scenarios but does not explicitly account for variations related to building height or occupancy patterns, which may influence roof thermal performance. Consequently, other building archetypes and occupant schedules should be considered in future studies to extend the findings.

5. Conclusions

This study demonstrates the effectiveness of a multi-step methodology combining experimental data and laboratory tests, Building Energy Model calibration, and advanced simulation processes to iteratively assess the performance of ventilated and permeable clay tile roofs in multiple building variants, climatic contexts, future scenarios, and adaptation pathways. The proposed workflow demonstrated both robustness and scalability in deriving reliable results and performance indicators from the calibrated building and roof models. Its structured methodology allows consistent application across a wide range of contexts, climatic conditions, and building typologies, enabling the evaluation of multiple retrofit scenarios. By providing quantitative insights into the thermal and energy performance of ventilated roof solutions, this approach offers valuable support to designers and decision-makers during the pre-retrofit assessment phase, facilitating informed decisions regarding the selection, optimization, and prioritization of intervention strategies. Moreover, the workflow's flexibility ensures that it can be adapted to future developments, including the integration of new building types, alternative roofing materials, or climate projections, thereby reinforcing its applicability in both research and practice.

The results clearly confirm the strong potential of the VPR technology, which outperforms a non-ventilated roof regardless of the climatic context and emission pathway, in reducing incoming heat and cooling demand already in the near future, as climate warming and cooling needs intensify.

This study highlights that the proposed VPR-HBR solution supports long-term climate mitigation benefits even in non-extreme climates without introducing additional impacts related to economic and material resource production, consumption, and disposal, typically associated with increased insulation levels. Unlike insulation-based envelope retrofit strategies, passive technologies such as VPR-HBR can contribute to improving building performance by enhancing natural ventilation mechanisms. Replacing roof tiles represents a complementary measure within a broader thermal retrofit strategy. This approach offers advantages in terms of life-cycle and end-of-life sustainability, confirming its role as a

climate-adaptive solution that can improve thermal comfort while limiting additional material and economic resources

Beyond energy performance benefits, the adoption of VPR-HBR also provides broader advantages by enhancing the thermal performance of existing buildings without increasing built volume or land occupation. This is particularly relevant in dense urban and Mediterranean contexts, where retrofit interventions must balance energy efficiency, environmental impacts in present and future scenarios, and land preservation.

Supplementary Materials: The following supporting information can be downloaded at: https://www.mdpi.com/article/10.3390/en19030670/s1, Table S1: Results of incoming heat fluxes across simulated building types, climates, cities and scenarios.

Author Contributions: Conceptualization, M.D., A.L. and E.D.G.; methodology, M.D. and A.L.; software, M.D. and A.L.; validation, M.D., E.D.G. and A.L.; formal analysis, M.D., A.L. and A.G.; investigation, A.L. and A.G.; resources, M.D. and E.D.G.; data curation, A.L. and A.G.; writing—original draft preparation, M.D. and A.L.; writing—review and editing M.D., A.L. and E.D.G.; visualization, A.L.; supervision, E.D.G.; project administration, E.D.G.; funding acquisition, E.D.G. All authors have read and agreed to the published version of the manuscript.

Funding: This work was supported by the Project LIFE SUPERHERO (LIFE19 CCA/IT/001194) "SUstainability and PERformaces for HEROTILE-based energy efficient roofs", performed with contributions from the European Union's LIFE Programme "Climate Change Adaptation".

Data Availability Statement: The dataset is available from the authors upon request.

Conflicts of Interest: The authors declare no conflicts of interest.

References

1. Magrini, A.; Lisot, A. Noise reduction interventions in the urban environment as a form of control of indoor noise levels. *Energy Procedia* **2015**, *78*, 1653–1658. [CrossRef]
2. Eurostat Housing in Europe. Available online: https://ec.europa.eu/eurostat/web/interactive-publications/housing-2025 (accessed on 1 December 2025).
3. Council of the European Union. *One Roof, Many Realities: Europe's Complex Housing Crisis*; Council of the European Union: Brussels, Belgium, 2025.
4. Salata, F.; Falasca, S.; Ciancio, V.; Curci, G.; de Wilde, P. Climate-change related evolution of future building cooling energy demand in a Mediterranean Country. *Energy Build.* **2023**, *290*, 113112. [CrossRef]
5. Raimundo, A.M.; Oliveira, A.V.M. Assessing the Impact of Climate Changes, Building Characteristics, and HVAC Control on Energy Requirements under a Mediterranean Climate. *Energies* **2024**, *17*, 2362. [CrossRef]
6. European Commission. *Assessing the Impact of Climate Change on Energy Demand in European Buildings*; European Commission: Brussels, Belgium, 2024.
7. Salvati, A.; Roura, H.C.; Cecere, C. Assessing the urban heat island and its energy impact on residential buildings in Mediterranean climate: Barcelona case study. *Energy Build.* **2017**, *146*, 38–54. [CrossRef]
8. Santamouris, M. Cooling the cities—A review of reflective and green roof mitigation technologies to fight heat island and improve comfort in urban environments. *Sol. Energy* **2014**, *103*, 682–703. [CrossRef]
9. Chen, Y.; Xiao, L.; Xu, H.; Wang, Z.; Mei, G.; Jiang, M.; Huang, S. Experimental and numerical analysis of thermal performance and energy consumption of ventilated green roof. *Energy Build.* **2025**, *330*, 115330. [CrossRef]
10. Gagliano, A.; Patania, F.; Nocera, F.; Galesi, A. Thermal performance of ventilated roofs during summer period. *Energy Build.* **2012**, *49*, 611–618. [CrossRef]
11. Di Giuseppe, E.; Pergolini, M.; Stazi, F. Numerical assessment of the impact of roof reflectivity and building envelope thermal transmittance on the UHI effect. *Energy Procedia* **2017**, *134*, 404–413. [CrossRef]
12. De Cristo, E.; Evangelisti, L.; Barbaro, L.; De Lieto Vollaro, R.; Asdrubali, F. A Systematic Review of Green Roofs' Thermal and Energy Performance in the Mediterranean Region. *Energies* **2025**, *18*, 2517. [CrossRef]
13. Cascone, S.; Rosso, F. Green roof as a passive cooling technique for the Mediterranean climate: An experimental study. *Riv. Tema* **2023**, *9*. [CrossRef]
14. Abu Qadourah, J. Energy efficiency evaluation of green roofs as a passive strategy in the mediterranean climate. *Results Eng.* **2024**, *23*, 102519. [CrossRef]

15. Di Giuseppe, E.; D'Orazio, M. Assessment of the effectiveness of cool and green roofs for the mitigation of the Heat Island effect and for the improvement of thermal comfort in Nearly Zero Energy Building. *Archit. Sci. Rev.* **2015**, *58*, 134–143. [CrossRef]
16. Di Giuseppe, E.; Sabbatini, S.; Cozzolino, N.; Stipa, P.; D'Orazio, M. Optical properties of traditional clay tiles for ventilated roofs and implication on roof thermal performance. *J. Build. Phys.* **2018**, *42*, 484–505. [CrossRef]
17. D'Orazio, M.; Di Perna, C.; Di Giuseppe, E. The effects of roof covering on the thermal performance of highly insulated roofs in Mediterranean climates. *Energy Build.* **2010**, *42*, 1619–1627. [CrossRef]
18. Lee, S.; Park, S.H.; Yeo, M.S.; Kim, K.W. An experimental study on airflow in the cavity of a ventilated roof. *Build. Environ.* **2009**, *44*, 1431–1439. [CrossRef]
19. Dimoudi, A.; Androutsopoulos, A.; Lykoudis, S. Summer performance of a ventilated roof component. *Energy Build.* **2006**, *38*, 610–617. [CrossRef]
20. Bottarelli, M.; Bortoloni, M.; Dino, G. Experimental analysis of an innovative tile covering for ventilated roofs (HERO tile). *Int. J. Low-Carbon Technol.* **2017**, *13*, 6–14. [CrossRef]
21. Baccega, E.; Bortoloni, M.; Bottarelli, M.; Dino, G.E.; Zannoni, G. Improving the Air Permeability of Ventilated Roofs. *Futur. Cities Environ.* **2022**, *8*, 8. [CrossRef]
22. Life Herotile. High Energy Resolution Tiles for Ventilated Roofs. 2016. Available online: https://www.lifeherotile.eu/it/ (accessed on 1 January 2024).
23. Life Superhero. Permeable and Ventilated Roofs for Sustainable Buildings. 2023. Available online: https://www.lifesuperhero.eu/ (accessed on 1 January 2024).
24. Griffith, B. A model for naturally ventilated cavities on the exteriors of opaque building thermal envelopes. In Proceedings of the Simbuilding Conference, Cambridge, MA, USA, 2–4 August 2006.
25. U.S. Department of Energy. *EnergyPlus Engineering Reference: Exterior Naturally Vented Cavity*; U.S. Department of Energy: Washington, DC, USA, 2024.
26. Walton, G.N. Airflow Network Models for Element-Based Building Airflow Modeling. *ASHRAE Trans.* **1989**, *95*, 611–620.
27. Di Giuseppe, E.; Maracchini, G.; D'Orazio, M. Implementation of Ventilated Permeable Roof Solutions in Urban Microclimate Models: A Preliminary Study. In Proceedings of the International Conference on Sustainability in Energy and Buildings, Madeira, Portugal, 18–20 September 2024; pp. 435–445. [CrossRef]
28. Heiranipour, M.; Favoino, F.; Gutierrez, M.J.; Avesani, S. Future Weather Dataset for Building Energy Simulations and Climate Resilience. 2024. Available online: https://build-up.ec.europa.eu/en/resources-and-tools/publications/future-weather-dataset-building-energy-simulations-and-climate (accessed on 1 January 2025).
29. Rodrigues, E.; Fernandes, M.S.; Carvalho, D. Future weather generator for building performance research: An open-source morphing tool and an application. *Build. Environ.* **2023**, *233*, 110104. [CrossRef]
30. Weathershift Inc. *Weathershift Heat: Adjusting Weather Files for Future Climatic Conditions*; Weathershift Inc.: Johns Creek, GA, USA, 2023.
31. Teixeira, J.P.; Silva, P.D.; da Pires, L.C.; Gaspar, P.D. Comparative Analysis of Passive Thermal Solutions for Building Resilience Under Future Climate Scenarios. *Energies* **2025**, *18*, 5693. [CrossRef]
32. Di Giuseppe, E.; Gianangeli, A.; Ferrari, B.; Latini, A.; D'Orazio, M. Roofs Passive Cooling Performance Through Air Permeability of Tiles: Development of a Standardized Laboratory Assessment Method. In Proceedings of the Lecture Notes in Civil Engineering, Singapore, 22–24 March 2025; Volume 2, pp. 564–570.
33. Di Giuseppe, E.; Maracchini, G.; Latini, A.; Bernardini, G.; D'Orazio, M. Building Management System and Data Sharing Platform for Passive Cooling Strategies Assessment and Users' Awareness Increase: Design and Application to a Social Housing Context in Italy. In *Sustainability in Energy and Buildings*; Littlewood, J.R., Jain, L., Howlett, R.J., Eds.; Springer Nature: Singapore, 2024; pp. 225–235. [CrossRef]
34. Loga, T.; Stein, B.; Diefenbach, N. TABULA building typologies in 20 European countries—Making energy-related features of residential building stocks comparable. *Energy Build.* **2016**, *132*, 4–12. [CrossRef]
35. Rosales, M.; Efthymiou, C.; Barmparesos, N.; Tasios, P.; Lissén, J.M.S.; Assimakopoulos, M.N. Identification of Reference Buildings in Mediterranean Countries: The HAPPEN Project Approach. *Appl. Sci.* **2022**, *12*, 5638. [CrossRef]
36. *UNI/TS 11300-1:2014*; Energy Performance of Buildings—Part 1: Evaluation of Energy Need for Space Heating and Cooling. ISO—International Organization for Standardization: Geneva, Switzerland, 2014. Available online: https://store.uni.com/en/uni-ts-11300-1-2014 (accessed on 1 January 2025).
37. *ISO 17772-1*; Energy Performance of Buildings—Indoor Environmental Quality—Part 1: Indoor Environmental Input Parameters for the Design and Assessment of Energy Performance of Buildings. ISO—International Organization for Standardization: Geneva, Switzerland, 2017.
38. *BS 5534:2014*; Slating and Tiling for Pitched Roofs and Vertical Cladding—Code of Practice. British Standard Institute: London, UK, 2014.

39. *ASTM C1570-22*; Standard Test Method for Wind Resistance of Concrete and Clay Roof Tiles (Air Permeability Method). ASTM: West Conshohocken, PA, USA, 2022. [CrossRef]
40. ASHRAE. *The 2001 ASHRAE Handbook*; Baird, J., Comstock, S., Eds.; ASHRAE: Atlanta, GA, USA, 2001.
41. D'Orazio, M.; Bernardini, G.; Di Giuseppe, E. Predict the priority of end-users' maintenance requests and the required technical staff through LSTM and Bi-LSTM recurrent neural networks. *Facilities* **2023**, *41*, 38–51. [CrossRef]
42. Manfren, M.; James, P.A.; Tronchin, L. Data-driven building energy modelling—An analysis of the potential for generalisation through interpretable machine learning. *Renew. Sustain. Energy Rev.* **2022**, *167*, 112686. [CrossRef]
43. Chen, Y.; Guo, M.; Chen, Z.; Chen, Z.; Ji, Y. Physical energy and data-driven models in building energy prediction: A review. *Energy Rep.* **2022**, *8*, 2656–2671. [CrossRef]
44. Nie, P.; Roccotelli, M.; Fanti, M.P.; Ming, Z.; Li, Z. Prediction of home energy consumption based on Gradient Boosting regression tree. *Energy Rep.* **2021**, *7*, 1246–1255. [CrossRef]
45. Di Persio, L.; Fraccarolo, N. Energy Consumption Forecasts by Gradient Boosting Regression Trees. *Mathematics* **2023**, *11*, 1068. [CrossRef]
46. Sauer, J.; Mariani, V.C.; dos Santos Coelho, L.; Ribeiro, M.H.D.M.; Rampazzo, M. Extreme gradient boosting model based on improved Jaya optimizer applied to forecasting energy consumption in residential buildings. *Evol. Syst.* **2022**, *13*, 577–588. [CrossRef]
47. R Studio. Available online: https://www.rstudio.com (accessed on 31 May 2021).
48. Martinez-Viol, V.; Urbano, E.M.; Delgado-Prieto, M.; Romeral, L. Automatic model calibration for coupled HVAC and building dynamics using Modelica and Bayesian optimization. *Build. Environ.* **2022**, *226*, 109693. [CrossRef]
49. Von Krannichfeldt, L.; Orehounig, K.; Fink, O. Integrating Physics-Based and Data-Driven Approaches for Probabilistic Building Energy Modeling. *Energy Build.* **2025**, *353*, 116838. [CrossRef]
50. *UNI EN ISO 6946:2018*; Building Components and Building Elements—Thermal Resistance and Thermal Transmittance—Calculation Methods. CEN—European Committe for Standardization: Brussels, Belgium, 2018. Available online: https://store.uni.com/en/uni-en-iso-6946-2018 (accessed on 1 June 2025).
51. Palyvos, J.A. A survey of wind convection coefficient correlations for building envelope energy systems' modeling. *Appl. Therm. Eng.* **2008**, *28*, 801–808. [CrossRef]
52. Lawrie, L.K.; Crawley, D.B. Development of Global Typical Meteorological Years (TMYx). 2022. Available online: https://climate.onebuilding.org/ (accessed on 1 June 2025).
53. Masoso, O.T.; Grobler, L.J. A new and innovative look at anti-insulation behaviour in building energy consumption. *Energy Build.* **2008**, *40*, 1889–1894. [CrossRef]
54. Gupta, V.; Deb, C. Envelope design for low-energy buildings in the tropics: A review. *Renew. Sustain. Energy Rev.* **2023**, *186*, 113650. [CrossRef]
55. Baba, F.M.; Ge, H.; Wang, L.; Zmeureanu, R. Do high energy-efficient buildings increase overheating risk in cold climates? Causes and mitigation measures required under recent and future climates. *Build. Environ.* **2022**, *219*, 109230. [CrossRef]
56. Beck, H.E.; McVicar, T.R.; Vergopolan, N.; Berg, A.; Lutsko, N.J.; Dufour, A.; Zeng, Z.; Jiang, X.; van Dijk, A.I.J.M.; Miralles, D.G. High-resolution (1 km) Köppen-Geiger maps for 1901–2099 based on constrained CMIP6 projections. *Sci. Data* **2023**, *10*, 724. [CrossRef] [PubMed]
57. Kottek, M.; Grieser, J.; Beck, C.; Rudolf, B.; Rubel, F. World map of the Köppen-Geiger climate classification updated. *Meteorol. Z.* **2006**, *15*, 259–263. [CrossRef] [PubMed]
58. Carver, S.; Mikkelsen, N.; Woodward, J. Long-term rates of mass wasting in Mesters Vig, northeast Greenland: Notes on a re-survey. *Permafr. Periglac. Process.* **2002**, *13*, 243–249. [CrossRef]